The Journal of Neuroscience, August 1, 2001, *21*(15):5824–5831

β and γ Frequency Synchronization by Dendritic GABAergic Synapses and Gap Junctions in a Network of Cortical Interneurons

János Szabadics,[1,2], Andrea Lorincz,[1] and Gábor Tamás[1,2]

[1]*Department of Comparative Physiology, University of Szeged, Szeged H-6726, Hungary, and* [2]*Medical Research Council Anatomical Neuropharmacology Unit, University Department of Pharmacology, University of Oxford, Oxford, OX1 3TH, United Kingdom*

Distinct interneuron populations innervate perisomatic and dendritic regions of cortical cells. Perisomatically terminating GABAergic inputs are effective in timing postsynaptic action potentials, and basket cells synchronize each other via gap junctions combined with neighboring GABAergic synapses. The function of dendritic GABAergic synapses in cortical rhythmicity, and their interaction with electrical synapses is not understood.

Using multiple whole-cell recordings in layers 2–3 of rat somatosensory cortex combined with light and electron microscopic determination of sites of interaction, we studied the interactions between regular spiking nonpyramidal cells (RSNPCs). Random samples of unlabeled postsynaptic targets showed that RSNPCs placed GABAergic synapses onto dendritic spines (53 $\pm$ 12%) and shafts (45 $\pm$ 10%) and occasionally somata (2 $\pm$ 4%). GABAergic interactions between RSNPCs were mediated by 4 $\pm$ 2 axodendritic synapses and phased postsynaptic activity at β frequency but were ineffective in phasing at γ rhythm. Electrical interactions of RSNPCs were transmitted via two to eight gap junctions between dendritic shafts and/or spines. Elicited at β and γ frequencies, gap junctional potentials timed postsynaptic spikes with a phase lag, however strong electrical coupling could synchronize presynaptic and postsynaptic activity. Combined unitary GABAergic and gap junctional connections of moderate strength produced β and γ frequency synchronization of the coupled RSNPCs.

Our results provide evidence that dendritic GABAergic and/or gap junctional mechanisms effectively transmit suprathreshold information in a population of interneurons at behaviorally relevant frequencies. A coherent network of GABAergic cells targeting the dendrites could provide a pathway for rhythmic activity spatially segregated from perisomatic mechanisms of synchronization.

Key words: interneuron; synchronization; dendrite; gap junction; GABA; network

Oscillatory activity in different frequency bands occurs in the EEG during various behavioral states in mammals, including humans (Niedermeyer and Lopes da Silva, 1993). Particular cortical rhythms are clearly stimulus- and task-specific (Buzsaki et al., 1983; Singer, 1993; Steriade et al., 1993). γ band EEG activity has been observed in the neocortex *in vivo* associated with a number of cognitive processes, such as perception or attentional mechanisms (Steriade et al., 1993, 1996; Lisman and Idiart, 1995; Mainen and Sejnowski, 1995; Singer and Gray, 1995; Buzsaki, 1996; Jefferys et al., 1996), and β rhythms at 20 Hz are related to voluntarily controlled sensorimotor actions (Salmelin et al., 1995). Cortical GABAergic mechanisms have been implicated in governing population activity (Lytton and Sejnowski, 1991; Buzsaki and Chrobak, 1995; Cobb et al., 1995; Traub et al., 1996; Fisahn et al., 1998). Electrical synapses play a role in neuronal synchrony (Christie et al., 1989; Draguhn et al., 1998; Mann-Metzer and Yarom, 1999), and gap junctional coupling can promote synchronous activity in connections of cortical interneurons (Galarreta and Hestrin, 1999; Gibson et al., 1999; Koos and Tepper, 1999; Tamás et al., 2000; Venance et al., 2000). The precise spatiotemporal cooperation of gap junctional coupling with GABAergic synapses between basket cells further enhances populational coherence (Tamás et al., 2000).

GABAergic cells subdivide the surface of their target neurons (Somogyi et al., 1998), but most experiments addressing synchronization either did not examine the location of the inputs or were focused on perisomatic mechanisms (Cobb et al., 1995; Gupta et al., 2000; Tamás et al., 2000). Recent evidence suggests that a delicate balance of perisomatic and dendritic inhibition is essential in maintaining normal cortical rhythmogenesis because a deficit in dendritic inhibition could reduce seizure threshold, whereas enhanced somatic inhibition would prevent the continuous occurrence of epileptiform activity (Cossart et al., 2001). A particular subcellular domain of GABAergic and/or electrical communication might result in compartmental interaction of synaptic and voltage-gated conductances, resulting in the domain-specific processing of subthreshold and suprathreshold operations. In this work we identified a population of neocortical interneurons with dendritic target preference, which forms a network interacting via gap junctions, and GABAergic synapses. Neurons of this network are capable of engaging coherent activity and can be activated by local pyramidal cells at β and γ frequencies.

MATERIALS AND METHODS

Electrophysiology. Slices were obtained from Wistar rats (postnatal day 18–25) and maintained as described (Tamás et al., 2000). Whole-cell

Received Feb. 8, 2001; revised May 8, 2001; accepted May 18, 2001.

This work was supported by the James S. McDonnell Foundation (Eastern European Science Initiative Grant 97-39), the Wellcome Trust, and the Hungarian Scientific Research Fund (D32815). G.T. was a János Bolyai Research Scholar during part of this project. We thank Prof. P. Somogyi for his comments on an earlier version of this manuscript.

J.S. and A.L. have contributed equally to this work.

Correspondence should be addressed to Dr. Gábor Tamás, University of Szeged, Department of Comparative Physiology, Középfasor 52, Szeged, H-6726, Hungary. E-mail: gtamas@sol.cc.u-szeged.hu.

patch clamp recordings were performed at ~35°C from concomitantly recorded pairs, triplets, or quadruplets of layer 2–3 putative interneurons and/or pyramidal cells as detailed previously (Tamás et al., 2000). Micropipettes (5–7 MΩ) were filled with (in mM) 126 K-gluconate, 4 KCl, 4 ATP-Mg, 0.3 GTP-NA_2, 10 HEPES, 10 creatine phosphate, and 8 biocytin, pH 7.25, 300 mOsm. Signals were filtered at 5 kHz, digitized at 10 kHz, and analyzed with Pulse software (Heka, Lambrech/Pfalz, Germany). Presynaptic cells were stimulated with brief (2 msec) suprathreshold pulses at 60 msec intervals (16.6 Hz) for the paired pulse protocol and at 19 and 37 Hz for the β and γ frequency phasing paradigm. Depression and facilitation of EPSPs or IPSPs fully develops only after four or more postsynaptic events, therefore we used 6–10 presynaptic cycles to test the effect of the use-dependent modification of PSPs on the phasing of postsynaptic activity. We applied the same paradigm throughout the study for consistency. Trains were delivered at >5 sec intervals, to minimize intertrial variability. During subthreshold paradigms, postsynaptic cells were held at −51 ± 4 mV membrane potential. For phasing trials, they were depolarized with constant current injections just above threshold to elicit firing. Unless specified, traces shown are averages of 30–200 episodes. The amplitude of postsynaptic events was defined as the difference between the peak amplitude and the baseline value measured before the PSP onset. Firing probability plots were constructed from 50–100 consecutive trials as follows: within the interval separating two presynaptic action potentials, postsynaptic spike latencies were measured from the peak of the preceding presynaptic action potential. Subsequently, the data were pooled from cycles according to the characteristics of the postsynaptic responses (see Results). Controls were collected before the onset of the presynaptic spike train using identical cycle duration, and data obtained during presynaptic activation were normalized to control. Data are given as mean ± SD. Mann–Whitney *U* test and Friedman test were used to compare datasets, and differences were accepted as significant if $p = 0.05$. Connections were classified by cluster analysis based on postsynaptic cell firing probability (Statistica for Windows; StatSoft, Tulsa, OK). Joining trees were constructed by Ward's method of amalgamation and were based on Euclidean distances.

Histology. Visualization of biocytin was performed as described (Buhl et al., 1994; Tamás et al., 1997). Three-dimensional light microscopic reconstructions were performed using Neurolucida (MicroBrightfield, Colchester, VT) with 100× objective; dendrogram constructions and synaptic distance measurements were aided by Neuroexplorer (MicroBrightfield) software. Dendrograms represent only the dendrites involved in the connections. Correlated light and electron microscopy was performed as described earlier (Buhl et al., 1994; Tamás et al., 1997).

RESULTS

Several hundred simultaneous dual, triple, and quadruple recordings of neurons in layers 2–3 of rat somatosensory cortex provided 28 RSNPCs to RSNPC connections and 12 pyramidal cell (PC) to RSNPC connections. RSNPCs were identified based on their physiological and anatomical properties (Cauli et al., 1997; Kawaguchi and Kubota, 1997; Cauli et al., 2000). Similar to RSNPCs identified earlier they responded to long (800 msec) depolarizing current pulses with a regular spiking firing pattern showing first to second spike amplitude reduction of 23 ± 11% and input resistance of 375 ± 117 MΩ (Fig. 1*A*). Local pyramidal cells elicited unitary EPSPs in RSNPCs with paired pulse depression ($n = 12$; amplitude of the first response, 1.24 ± 1.25 mV; paired pulse ratio, 56 ± 14%) (Porter et al., 1998). The dendrites of RSNPCs originated from the two poles of their elongated somata (Figs. 2*C*, 3*B,C*, 4*C*) and were sparsely spiny (Fig. 3*E,F*). The axons formed a dense cloud around the dendritic tree and sent a loose bundle of radial branches spanning all layers of the cortex (Fig. 3*B*). High-order axonal branches of RSNPCs ran radially and branched rectangularly (Figs. 2*C*, 4*C*). Electron microscopic random samples of unlabeled postsynaptic targets ($n = 267$) taken from layers 2–5 showed that RSNPCs ($n = 10$) innervated dendritic spines (53 ± 12%) and shafts (45 ± 10%) and occasionally somata (2 ± 4%) (Fig. 1*B*). Detailed analysis of serial sections revealed that only 44 ± 21% of postsynaptic targets identified as dendritic spines received asymmetrical synapses.

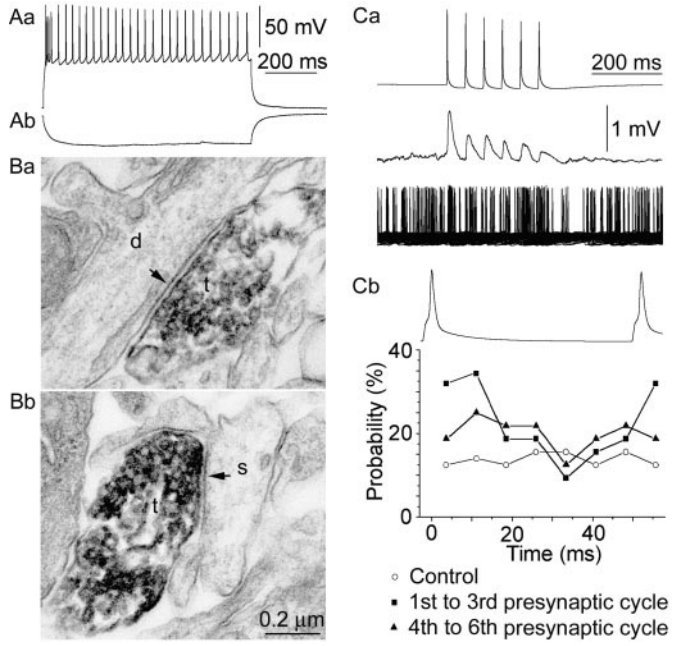

Figure 1. Identification of RSNPCs and modulation of their firing by presynaptic β and γ frequency activity of layer 2/3 pyramidal cells. Response of an RSNPC to a depolarizing (*Aa*; 180 pA) and hyperpolarizing (*Ab*; −100 pA) current pulse. Biocytin-filled axon terminals (*t*) of RSNPCs formed synapses (*arrows*) with unlabeled dendritic (*d*) shafts (*Ba*) and spines (*s*) (*Bb*). *Ca*, Pyramidal cell firing at 19 Hz (*top*) elicited EPSPs showing marked activity-dependent depression in a postsynaptic RSNPC (*middle*). Subsequently, the postsynaptic cell was tonically depolarized to fire at a frequency of ~4 Hz (bottom, 50 consecutive superimposed sweeps). *Cb*, Firing probability plot of the postsynaptic RSNPC during a representative presynaptic action potential cycle shows that only the first three cycles were effective in phasing postsynaptic activity at β frequency.

Rhythmic activation of RSNPCs by local PCs was tested in six pairs at β and γ frequencies (19 and 37 Hz, respectively). Presynaptic PC firing at both frequencies resulted in use-dependent depression of postsynaptic unitary EPSPs in all RSNPCs (Fig. 1*Ca*). Presynaptic spike trains at β rhythm increased the mean frequency of ongoing postsynaptic firing to 125 ± 14% of the control value, respectively (from 4.2 ± 1.4 to 5.3 ± 1.7 Hz) (Figs. 1*Ca*, 5*B*). β frequency presynaptic activation entrained postsynaptic firing during the first three presynaptic cycles. During these cycles, postsynaptic firing probability was significantly higher in the first three bins (0–22.3 msec) after the preceding presynaptic spike than later (Figs. 1*Cb*, 5*B*). In parallel with the depression of unitary EPSPs, phasing effectiveness of PCs on RSNPC firing faded during the rest of presynaptic activity (Fig. 1*Cb*). Similar results were obtained at γ frequency PC activation (Fig. 5*B*). When driving the PCs at 37 Hz, the mean firing rate of postsynaptic RSNPCs was accelerated to 132 ± 26% of the control, and entrainment of postsynaptic firing was limited to the first two ($n = 3$ pairs) or three ($n = 3$ pairs) presynaptic cycles. During these cycles, postsynaptic firing probability was significantly higher in the second and third bins (7.4–22.3 msec) after the preceding presynaptic spike than during the rest of bins (Figs. 1*Cb*, 5*B*).

We identified GABAergic, electrical, and combined GABAergic and electrical connections between RSNPCs. In pairs of RSNPCs connected by chemical synapses only ($n = 12$), light-microscopic analysis of six fully visualized cell pairs indicated 4 ± 2 close appositions between presynaptic axons and postsynaptic

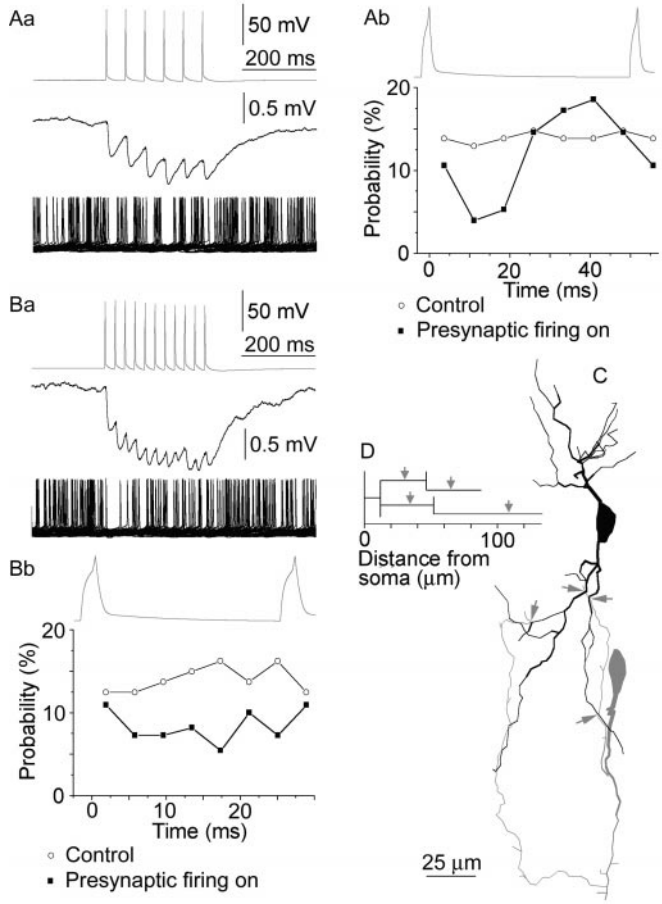

Figure 2. Dendritic GABAergic synapses can phase somatic action potential generation in a RSNPC to RSNPC connection. Data acquired from the presynaptic and postsynaptic cells are presented in *gray* and *black*, respectively. *Aa*, Repetitive presynaptic firing at 19 Hz (*top*) resulted in the summation of unitary IPSPs followed by the stabilization of their amplitude in the postsynaptic cell (*middle*). When tonically depolarizing to fire, the postsynaptic RSNPC became effectively entrained with a phase lag of ~41 msec throughout the entire duration of presynaptic activity (*bottom*, 50 consecutive sweeps). *Ab*, Distribution of postsynaptic firing probability during a representative presynaptic action potential cycle. *Ba*, Repeating the experiment shown in *A* with 37 Hz presynaptic activation (*top*) resulted in early summation and subsequent stabilization of IPSP amplitude (*middle*). GABAergic synapses between RSNPCs were not effective in phasing postsynaptic firing at γ frequency as shown by 50 consecutive superimposed sweeps (*Ba, bottom*) and average firing probability distribution during a presynaptic cycle (*Bb*). *C*, Distribution of GABAergic input on the dendritic tree of the postsynaptic RSNPC (*black*). The axon of the presynaptic cell (*gray*) innervated secondary and tertiary dendrites (*arrows*), as detected by light microscopy. *D*, Dendrogram representing the innervated dendritic segments of the postsynaptic cell and three-dimensional distances of synapses (*arrows*).

dendrites at a mean distance of 63 ± 28 μm from the somata (Fig. 2*C,D*). All GABAergic connections were unidirectional between RSNPCs in our sample. Measured at −51 ± 3 mV membrane potential, unitary IPSPs between RSNPCs were 0.54 ± 0.23 mV in amplitude ($n = 12$). Bicuculline completely abolished the responses (20 μM; $n = 3$). Repetitive presynaptic firing at 19 and 37 Hz resulted in the summation of postsynaptic unitary IPSPs followed by the stabilization of their amplitude ~ 198 ± 49 and 238 ± 57% of the amplitude of averaged single events, respectively ($n = 6$) (Fig. 2*Aa,Ba*). Presynaptic spike trains (19 Hz) decreased the mean frequency of spontaneous postsynaptic firing to 79 ± 18% of the control value (from 4.6 ± 1.9 to 3.6 ± 1.7 Hz). Postsynaptic firing was entrained for the entire duration of presynaptic activation. Postsynaptic firing probability was significantly smaller in the second and third bins (7.4–22.3 msec) after the preceding presynaptic spike than during the first, sixth, and seventh bins (0–7.4 and 37.1–52 msec) in a cycle (Figs. 2*Ab*, 5*C*). γ frequency presynaptic activation (37 Hz) could decrease the mean postsynaptic discharge rate from 4.7 ± 1.7 to 3.2 ± 1.3 Hz (69 ± 12%) but was not effective in phasing postsynaptic action potential generation (Figs. 2*B*, 5*C*).

The second class of RSNPC to RSNPC connections was mediated by electrical synapses ($n = 12$). Light-microscopic mapping in five fully recovered pairs detected 3 ± 3 close appositions (range, 2–8) exclusively between dendrites at a mean distance of 77 ± 34 μm from the somata (Fig. 3*B–D*). Electron microscopic analysis of the suspected coupling sites was performed in one cell pair, leading to the identification of eight gap junctions in the connection at dendritic distances of 72 ± 16 μm (cell 1) and 63 ± 36 μm (cell 2) from the somata (Fig. 3*C–H*). Two gap junctions were established between dendritic spines, one between a spine and a dendritic shaft, and four gap junctions linked dendritic shafts. Analysis of serial ultrathin sections showed in all four dendritic shaft to dendritic shaft cases that the junctional region was composed of the gap junction and an immediately adjacent patch of membranes running parallel for 0.3–0.9 μm at a rigid distance of 21–25 nm (Fig. 3*G,H*). The latter value is characteristic of desmosomes and/or synaptic clefts, but the electron opaque reaction end product prevented further identification of junctional components.

All electrical connections between RSNPCs were reciprocal. Gap junctional potentials (GJPs) showed a relatively wide range in amplitude (0.07–2.42 mV; 0.62 ± 0.74 mV) at −50 ± 3 mV membrane potential and had an average duration of 19.6 ± 8.2 msec, as measured at half amplitude. They followed presynaptic action potentials with a delay of 0.40 ± 0.26 msec, measured as the period spanning the maximal rates of rise of the presynaptic action potential and the GJP, respectively. The average amplitude ratio (coupling coefficient) for GJPs and presynaptic potentials was 0.66 ± 0.83% (range, 0.04–2.58%) and 4.6 ± 3.1% (range, 2.4–10.6%) when eliciting action potentials and applying long current steps (200 pA, 300 msec duration) in the first neuron to elicit a response in the second neuron. Coupling strength was similar in both directions and did not show voltage dependence between −80 and −40 mV postsynaptic membrane potential ($n = 4$). Both amplitudes and kinetics of GJPs remained unchanged during repetitive presynaptic firing (Fig. 3*Aa,Ia*). The effect on unitary GJPs on postsynaptic suprathreshold activity was investigated at 19 and 37 Hz in six connections. For a given pair, timing of postsynaptic firing was similar at both frequencies tested, and members of a pair phased one another with similar efficacy regardless of the direction. In four of six pairs, 19 Hz presynaptic activation accelerated the mean firing rate of postsynaptic RSNPCs to 120 ± 10% of the control. Postsynaptic firing probability was significantly higher in the first two bins (0–14.9 msec) after the preceding presynaptic spike than during the last three bins (29.7–52 msec) of a cycle (Fig. 5*D*). GJPs arriving at γ frequency increased ongoing postsynaptic firing, and firing probability was significantly higher in the second bin (3.9–7.7 msec after the presynaptic spike) than in the rest of bins in a cycle (Figs. 3*I*, 5*D*). In the two pairs with the highest coupling ratios and numbers of gap junctions, GJPs synchronized presynaptic and postsynaptic firing at β and γ frequencies with no apparent

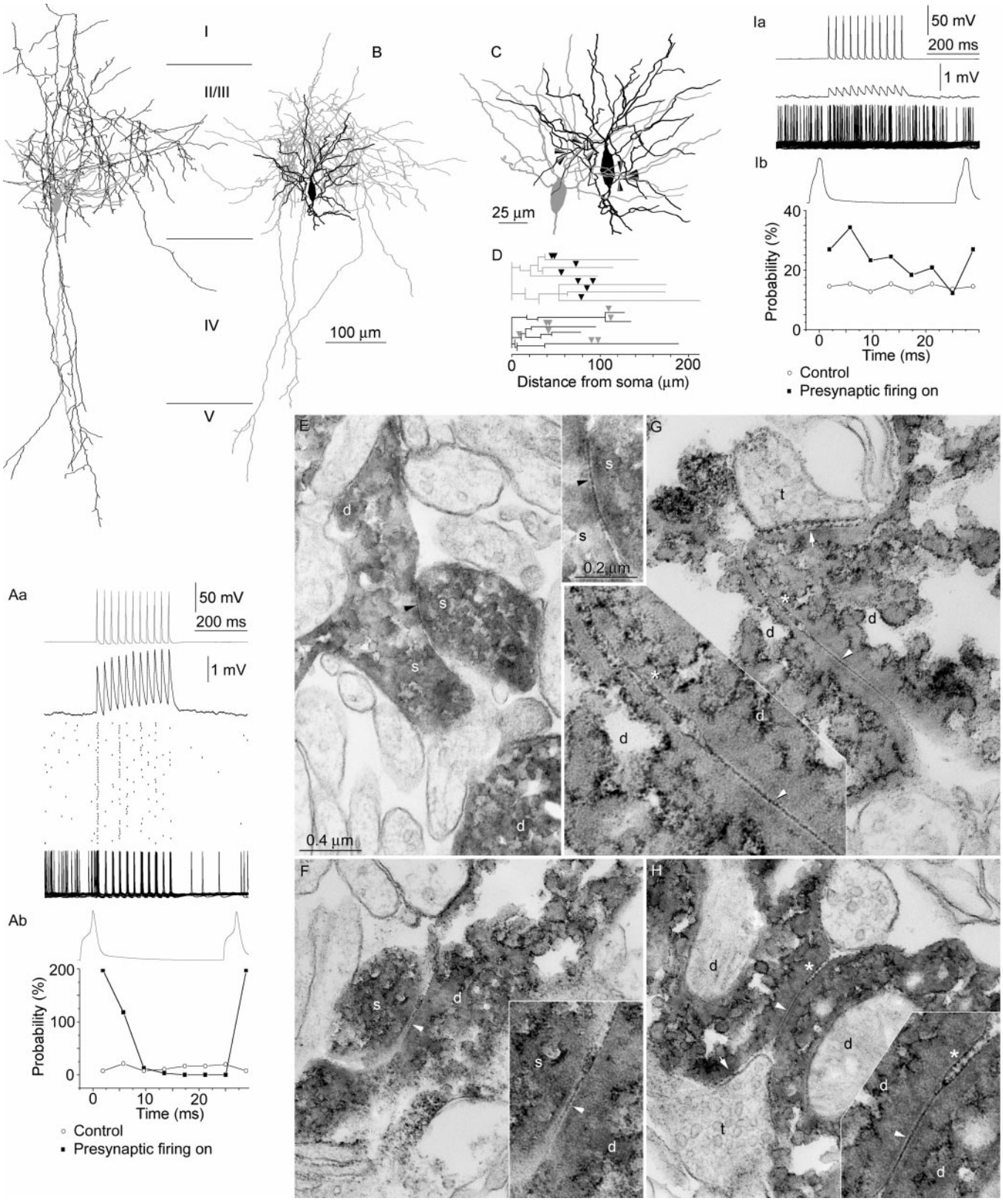

Figure 3. Gap junctional connections between RSNPCs. *A–H*, Synchronization of a pair of RSNPCs by strong gap junctional coupling. *Aa*, Electrical coupling produces gap junctional potentials of relatively stable amplitude (*middle*) in response to presynaptic trains of action potentials delivered at 37 Hz (*top*). The scattergram represents the timing of individual action potentials in 50 consecutive trials during tonic depolarization of the postsynaptic cell. Robust gap junctional coupling was highly potent in synchronizing presynaptic and postsynaptic activity, as shown by the overlay of the 50 trials (*bottom*). *Ab*, Distribution of postsynaptic action potentials relative to a presynaptic cycle. *B–H*, Anatomical correlates of the electrical interaction shown in *A*. *B*, Reconstructions of RSNPC 1 (soma and dendrites, *gray*; axon, *black*) and RSNPC 2 (soma and dendrites, *black*; axon, *gray*) cells. Cortical layers are indicated in the *middle* (*I–V*). *C*, Relative arrangement of somata and dendrites of the coupled cells. Electron micro- (*Figure legend continues*.)

phase lag (bin width, 3.9 msec) and a relatively narrow temporal scatter of action potentials (Fig. 3*A*).

Six RSNPC to RSNPC connections were mediated by combined GJPs and IPSPs. The GABAergic component of all dual electrical and chemical connections was unidirectional. Light microscopic mapping of three fully recovered pairs revealed that gap junctions as well as chemical synapses were located in the dendritic domain of the postsynaptic cells at a mean distance of 59 ± 21 and 75 ± 18 μm from the somata, respectively. Detailed electron microscopic analysis of one pair confirmed such arrangement of connections and identified two gap junctions between dendritic shafts (one of them showing rigid widening of extracellular space adjacent to the gap junction) and three GABAergic synapses on dendrites (Fig. 4*C–F*). Postsynaptic responses were composed of GJPs followed by short-latency IPSPs of stable amplitude (Fig. 4*A,B*). Presynaptic spike trains at 19 and 37 Hz decreased the mean frequency of ongoing postsynaptic firing to 91 ± 11% and 84 ± 8% of control values, respectively (from 5.08 ± 1.19 to 4.62 ± 1.13 Hz and from 5.22 ± 1.34 to 4.38 ± 1.27 Hz). After the onset of presynaptic spike trains, postsynaptic firing was instantly synchronized at β and γ frequencies, with maximal postsynaptic action potential probability in the first bin (bin widths, 7.4 and 3.9 msec) (Figs. 4*Ab,Bb*, 5*E*). Firing occurred synchronously in the coupled cells during the entire length of presynaptic activation.

Cluster analysis of postsynaptic firing probability in response to β and γ frequency presynaptic firing resulted in the clear delineation of controls, connections mediated by IPSPs, and combined electrical and GABAergic coupling (Fig. 5*F*). Interactions via moderate gap junctional coupling and EPSPs clustered together (Fig. 5*F*), but the two electrical connections mediated by powerful coupling formed a separate group at both frequencies (data not shown).

DISCUSSION

We have identified a novel interneuronal network in the cortex interconnected by electrical and GABAergic synapses. RSNPCs form dendritic gap junctions with other RSNPCs and establish GABAergic synapses on the dendritic domain of postsynaptic cells. Electrical, GABAergic, or combined GABAergic and gap junctional signals targeted to the dendrites are capable of timing somatic action potential generation in the network of RSNPCs at behaviorally relevant frequencies.

Interneurons forming the network identified here are distinct of GABAergic cell classes known to form electrically coupled networks in the cortex (Galarreta and Hestrin, 1999; Gibson et al., 1999; Tamás et al., 2000; Venance et al., 2000). The regular spiking firing pattern in combination with depressor unitary EPSPs demarcate RSNPCs both from fast-spiking cells and from low-threshold spiking and bitufted cells (Reyes et al., 1998; Gibson et al., 1999), and these electrophysiological parameters are similar to those of vasoactive intestinal polypeptide-immunoreactive interneurons (Kawaguchi and Kubota, 1996; Cauli et al., 2000). In agreement with earlier results (Kawaguchi and Kubota, 1997; Tamás et al., 1997), we have found that RSNPCs place symmetrical synapses onto dendritic spines and shafts. These results would identify RSNPCs as double bouquet cells (Somogyi and Cowey, 1981; Tamás et al., 1997), but the finding that only less than half of postsynaptic targets identified as dendritic spines received asymmetrical synapses questions the origin of postsynaptic dendritic appendages. Although the synaptology of interneuronal spines are not known, the spines receiving excitatory synapses are most likely originate from pyramidal dendrites; the ones receiving GABAergic innervation only could belong to pyramidal cells as well as GABAergic interneurons. Double bouquet cells target other GABAergic neurons (Tamás et al., 1998), there are known types of interneuron preferentially innervating other GABAergic cells in the rat (Gulyas et al., 1996; Meskenaite, 1997), and the distinction between these classes is not yet clear. Gap junctions between RSNPCs also connect dendritic shafts and spines and, moreover, GABAergic synapses and gap junctions are placed at similar distances from the soma of RSNPCS. Therefore, similarly to the network of cortical basket cells (Tamás et al., 2000), chemical and electrical synapses target the same subcellular domain of RSNPCs equalizing the time required for postsynaptic signal propagation. Accurate spatial integration could be further promoted by juxtaposition of gap junctions, dendrodendritic synapses, and/or desmosomes found between smooth dendritic shafts in the primate motor cortex (Sloper and Powell, 1978) and between parvalbumin-immunoreactive dendrites in the hippocampus (Fukuda and Kosaka, 2000). We found a rigid widening of the extracellular space next to the gap junctions in six of five contacts between dendritic shafts of RSNPCs, but our method for the visualization of functionally coupled cells did not allow the differentiation of desmosomes and dendrodendritic synaptic junctions.

We provide evidence that dendritically targeted GABAergic synapses are effective in timing somatic action potentials in the postsynaptic RSNPCs. Mechanisms underlying such phasing are not yet known. GABAergic cell types elicit IPSCs and IPSPs with remarkably different kinetics (Gupta et al., 2000), which could reflect distinct postsynaptic receptor properties (Draguhn et al., 1990; Mody et al., 1994). Currents activated by hyperpolarization (I_h) are present in RSNPCs, but not as prominent as in pyramidal cells and bitufted cells (our unpublished data; Cauli et al., 2000). Therefore, activation and/or deinactivation of other voltage-gated cation conductances and/or by passive dendritic properties could be the major factors in shaping the relatively fast decay of IPSPs. Dendritic GABAergic synapses between RSNPCs are able to phase postsynaptic cells in the β frequency band, which is clearly faster than the theta frequency range of

←

scopically identified gap junctions (*arrowheads*) mediating the interaction between the coupled cells were found on dendrites. *D*, Dendrograms representing three-dimensional dendritic distances of gap junctions (*arrowheads*). *E–H*, Examples of the eight electron microscopically identified gap junctions (*arrowheads*) between the RSNPCs. *Insets* show the junctional regions at higher magnification. *E*, Dendritic spines (*s*) establish a gap junction between RSNPC 1 (*left*) and RSNPC 2 (*right*; *d*, parent dendritic shafts). *F*, Gap junction between a dendritic spine (*s*) of RSNPC 1 and a dendritic shaft (*d*) of RSNPC 2. *G–H*, Dendritic shafts of RSNPC1 and 2 (*d*) form gap junctions. Note the parallel membrane appositions with widened extracellular space of 21–25 nm (*) adjacent to both dendrodendritic gap junctions. Synaptic junctions are indicated (*arrows*) between unlabeled terminals (*t*) and the dendrites of RSNPC 1. Electrical coupling between RSNPCs entrained postsynaptic firing with a phase lag in most pairs examined. *Ia*, Presynaptic action potentials at 37 Hz (*top*) elicited gap junctional potentials of moderate amplitude in the postsynaptic cell (*middle*, same scale as in *Aa*). When tonically depolarizing the postsynaptic RSNPC to fire, postsynaptic action potentials became entrained with a phase lag of ~6 msec throughout the entire duration of presynaptic activity (50 consecutive sweeps). *Ib*, Distribution of postsynaptic firing probability during a representative presynaptic action potential cycle.

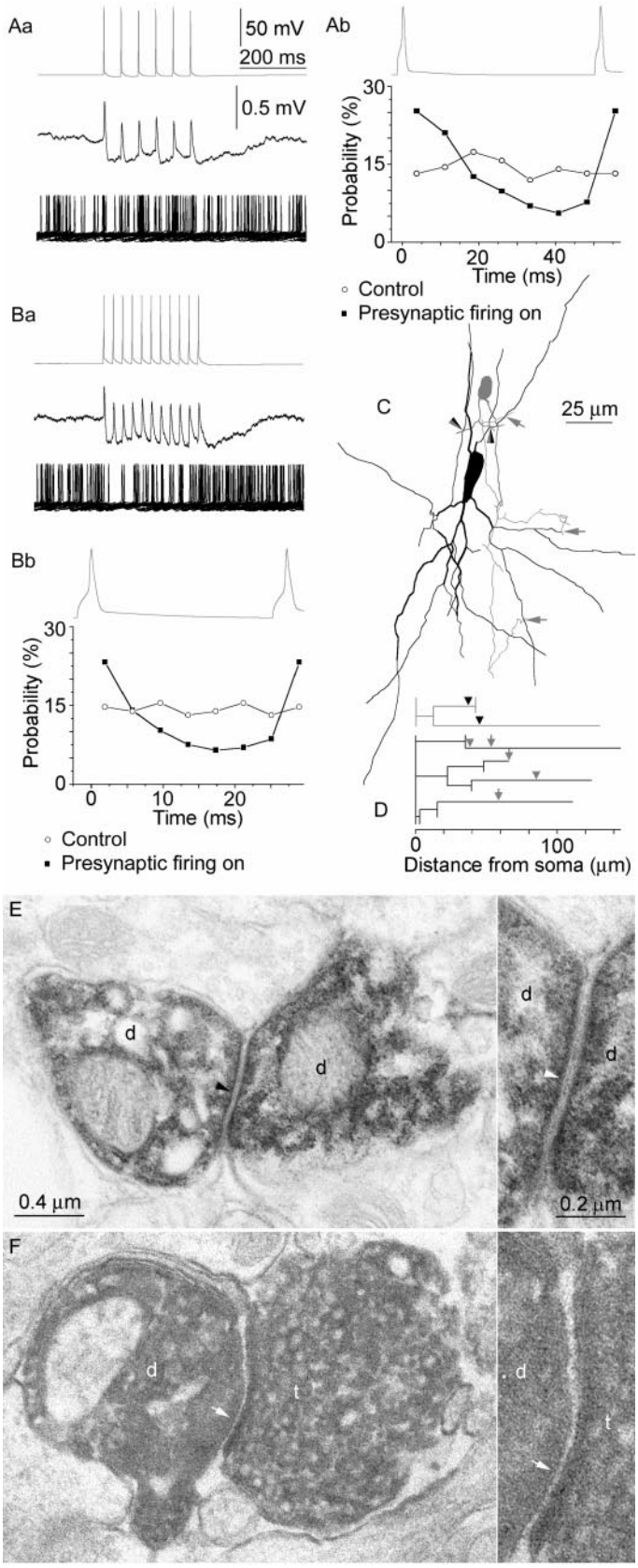

Figure 4. Synchronization of RSNPCs through combined unitary gap junctions and GABAergic synapses targeting the dendritic domain. Data obtained from the presynaptic and postsynaptic cells are presented in *gray* and *black*, respectively. *Aa–Bb*, Presynaptic action potentials evoked at 19 and 37 Hz (*Aa, Ba, top*) elicited spikelets followed by short-latency IPSPs in the postsynaptic neuron (*middle*). Dual coupling of moderate strength synchronized presynaptic and postsynaptic firing, as shown by 50 consecutive trials during tonic depolarization of the postsynaptic cell (*Aa, Ba, bottom*) and the probability plots of postsynaptic firing during a representative presynaptic cycle (*Ab, Bb*). *C*, The route of presynaptic dendrites and axons (*gray*) to gap junctions (*arrowheads*) and GABAergic synapses (*arrows*) on the postsynaptic cell (*black*). The dendrites and axons of the presynaptic cell are truncated for clarity. *D*, Dendrograms representing the dendritic branches of the two RSNPCs involved in the connections and three-dimensional distances of the sites of interaction. *E, F*, Examples of the two electron microscopically identified gap junctions and the three GABAergic synapses between the RSNPCs. *Insets* on the *right* show the junctional regions at higher magnification. *E*, Gap junction (*arrowhead*) between dendritic shafts (*d*) of the presynaptic (*right*) and postsynaptic (*left*) cell. *F*, A terminal (*t*) of the presynaptic cell establishes a synaptic junction (*arrow*) on a dendritic shaft (*d*) of the postsynaptic cell.

rebound activation detected in connections mediated by perisomatically placed GABAergic synapses on pyramidal cells (Cobb et al., 1995) as well as on interneurons (Tamás et al., 2000). The rebound activation might be even faster *in vivo*, when the input resistance of the cells is likely to be lower because of ongoing background synaptic activity. This could improve phasing between RSNPCs in the γ frequency band. Theta and β/γ rhythms are linked to distinct behaviors (Buzsaki et al., 1983; Singer, 1993; Steriade et al., 1993), and our results suggest that diverse populations of GABAergic cells might be differentially involved in cortical network operations during a particular activity.

Unitary EPSPs could initiate firing in RSNPCs with latencies slightly longer to what has been found in hippocampal interneurons (Fricker and Miles, 2000). These authors measured the timing of spikes elicited from just subthreshold membrane potentials, but we have tested the effectiveness of GJPs and EPSPs (and IPSPs and dual coupling) on spontaneous ongoing firing. The set of voltage-gated conductances active at subthreshold membrane potentials and during spontaneous repetitive firing is likely to be different and might explain the discrepancy. The amplitude of GJPs versus EPSPs might also influence the immediacy of spikes after the onset of the postsynaptic potentials by activating different amounts and or populations of voltage-gated channels. In addition to spike triggering, suprathreshold activity of RSNPCs can be rhythmically timed with a phase lag by neighboring pyramidal cells in the β and γ frequency range.

Strong bidirectional electrical coupling could produce synchronization of RSNPCs, but on average, combined chemical and electrical unitary connections were most effective in synchronizing presynaptic and postsynaptic firing. In our sample, all GABAergic connections were unidirectional between RSNPCs including the GABAergic component of dual electrical and chemical connections. The implications of unidirectional GABAergic coupling in combination with reciprocal gap junctional connections are not clear. RSNPCs are embedded into a network interconnected by chemical, electrical, and dual unitary connections, and a particular postsynaptic cell is likely to receive convergent GJPs and IPSPs from some RSNPCs that might be precisely synchronized by dual coupling. This scenario suggests that dual connections would rule the operation of RSNPCs at the network level. Preferred rhythms of RSNPC population oscillations might be in the β and probably γ frequency band set by the timing of rebound activation after unitary IPSPs within the network. Coherent output of RSNPCs could provide a powerful dendritic pathway of rhythmic information processing spatially

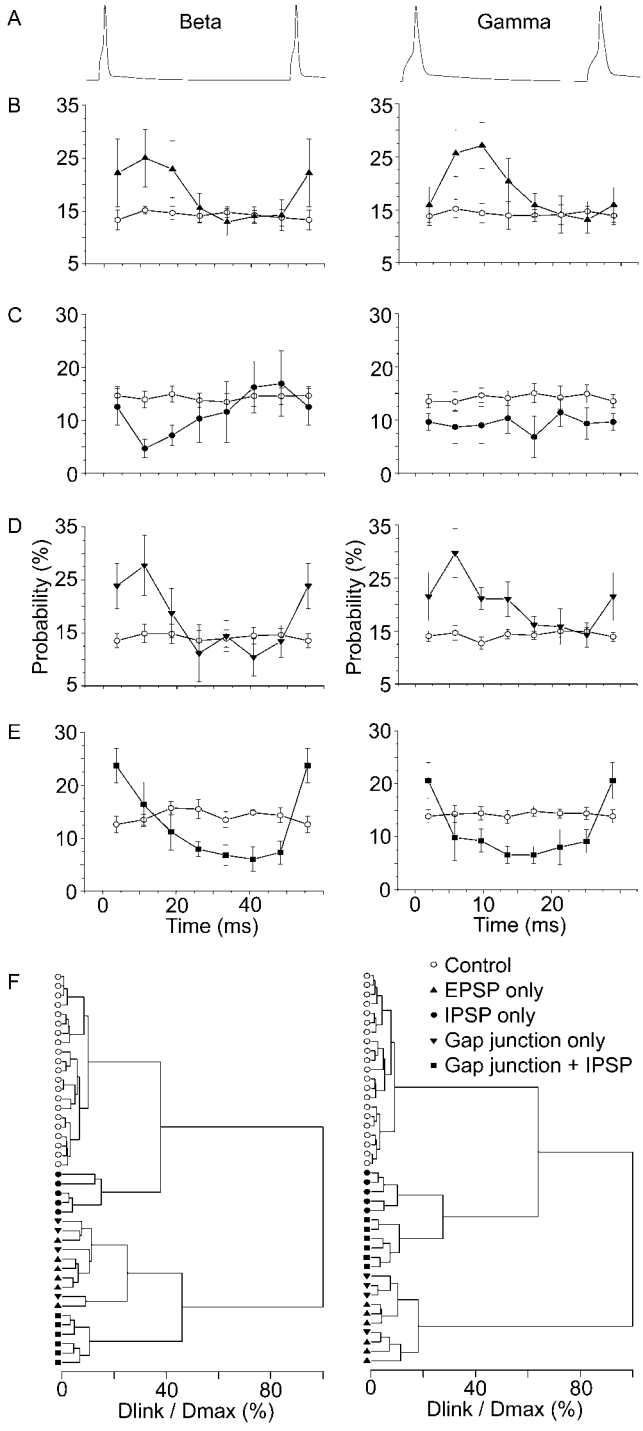

Figure 5. Differential entrainment of suprathreshold activity by inputs targeting RSNPCs. *A*, Representative presynaptic cycles at β (19 Hz) and γ (37 Hz) frequency. *B–E*, Firing probability plots of postsynaptic RSNPCs during representative presynaptic action potential cycles shown in *A* when EPSPs (*B*; $n = 6$), IPSPs (*C*; $n = 5$), gap junctions (*D*; $n = 4$), and dual electrical and GABAergic synapses (*E*; $n = 6$) mediated unitary interactions. In pyramid-to-RSNPC connections, only the first two presynaptic cycles entrained postsynaptic firing in all pairs; the rest of the cycles are not shown (Fig. 1*Cb*). The two electrical-only connections with the highest coupling ratios and numbers of gap junctions are not presented in this figure (see Results and Fig. 3*A–H*). *F*, Cluster analysis of the data presented in *B–E*. Controls, connections mediated by IPSPs, and combined electrical and GABAergic coupling form distinct groups, interactions through gap junctions only, and EPSP overlap. *Dlink/Dmax,* Linking and maximal Euclidean distances.

and temporally segregated from perisomatic mechanisms of synchronization. The cooperation of GABAergic synapses and gap junctions appears to be limited to a single population of interneurons (Galarreta and Hestrin, 1999; Gibson et al., 1999; Tamás et al., 2000; Venance et al., 2000), therefore synchronization might be more prominent within populations than across different interneuron types. This might explain the effectiveness of soma and dendrite targeting interneurons in timing postsynaptic activity of pyramidal cells though a precisely synchronized, robust, but perisomatically and dendritically channeled GABAergic flow of information.

REFERENCES

Buhl EH, Halasy K, Somogyi P (1994) Diverse sources of hippocampal unitary inhibitory postsynaptic potentials and the number of synaptic release sites. Nature 368:823–828.
Buzsaki G (1996) The hippocampo-neocortical dialogue. Cereb Cortex 6:81–92.
Buzsaki G, Chrobak JJ (1995) Temporal structure in spatially organized neuronal ensembles: a role for interneuronal networks. Curr Opin Neurobiol 5:504–510.
Buzsaki G, Leung L-W, Vanderwolf CH (1983) Cellular bases of hippocampal EEG in the behaving rat. Brain Res Rev 6:139–171.
Cauli B, Audinat E, Lambolez B, Angulo MC, Ropert N, Tsuzuki K, Hestrin S, Rossier J (1997) Molecular and physiological diversity of cortical nonpyramidal cells. J Neurosci 17:3894–3906.
Cauli B, Porter JT, Tsuzuki K, Lambolez B, Rossier J, Quenet B, Audinat E (2000) Classification of fusiform neocortical interneurons based on unsupervised clustering. Proc Natl Acad Sci USA 97:6144–6149.
Christie MJ, Williams JT, North RA (1989) Electrical coupling synchronizes subthreshold activity in locus coeruleus neurons in vitro from neonatal rats. J Neurosci 9:3584–3589.
Cobb SR, Buhl EH, Halasy K, Paulsen O, Somogyi P (1995) Synchronization of neuronal activity in hippocampus by individual GABAergic interneurons. Nature 378:75–78.
Cossart R, Dinocourt C, Hirsch JC, Merchan-Perez A, De Felipe J, Esclapez M, Bernard C, Ben-Ari Y (2001) Dendritic but not somatic GABAergic inhibition is decreased in experimental epilepsy. Nat Neurosci 4:52–62.
Draguhn A, Verdorn TA, Ewert M, Seeburg PH, Sakmann B (1990) Functional and molecular distinction between recombinant rat GABAA receptor subtypes by Zn^{2+}. Neuron 5:781–788.
Draguhn A, Traub RD, Schmitz D, Jefferys JG (1998) Electrical coupling underlies high-frequency oscillations in the hippocampus in vitro. Nature 394:189–192.
Fisahn A, Pike FG, Buhl EH, Paulsen O (1998) Cholinergic induction of network oscillations at 40 Hz in the hippocampus in vitro. Nature 394:186–189.
Fricker D, Miles R (2000) EPSP amplification and the precision of spike timing in hippocampal neurons. Neuron 28:559–569.
Fukuda T, Kosaka T (2000) Gap junctions linking the dendritic network of GABAergic interneurons in the hippocampus. J Neurosci 20:1519–1528.
Galarreta M, Hestrin S (1999) A network of fast-spiking cells in the neocortex connected by electrical synapses. Nature 402:72–75.
Gibson JF, Beierlein M, Connors BW (1999) Two networks of electrically coupled inhibitory neurons in neocortex. Nature 402:75–79.
Gulyas AI, Hajos N, Freund TF (1996) Interneurons containing calretinin are specialized to control other interneurons in the rat hippocampus. J Neurosci 16:3397–3411.
Gupta A, Wang Y, Markram H (2000) Organizing principles for a diversity of GABAergic interneurons and synapses in the neocortex. Science 287:273–278.
Jefferys JGR, Traub RD, Whittington MA (1996) Neuronal networks for induced "40 Hz" rhythms. Trends Neurosci 19:202–208.
Kawaguchi Y, Kubota Y (1996) Physiological and morphological identification of somatostatin- or vasoactive intestinal polypeptide-containing cells among GABAergic cell subtypes in rat frontal cortex. J Neurosci 16:2701–2715.
Kawaguchi Y, Kubota Y (1997) GABAergic cell subtypes and their synaptic connections in rat frontal cortex. Cereb Cortex 7:476–486.
Koos T, Tepper JM (1999) Inhibitory control of neostriatal projection neurons by GABAergic interneurons. Nat Neurosci 2:467–472.
Lisman JE, Idiart MAP (1995) Storage of 7±2 short-term memories in oscillatory subcycles. Science 267:1512–1515.
Lytton WW, Sejnowski TJ (1991) Simulations of cortical pyramidal neurons synchronized by inhibitory interneurons. J Neurophysiol 66:1059–1079.
Mainen ZF, Sejnowski TJ (1995) Reliability of spike timing in neocortical neurons. Science 268:1503–1506.

Mann-Metzer P, Yarom Y (1999) Electrotonic coupling interacts with intrinsic properties to generate synchronized activity in cerebellar networks of inhibitory interneurons. J Neurosci 19:3298–3306.
Meskenaite V (1997) Calretinin-immunorective local circuit neurons in area 17 of the cynomolgus monkey, *Macaca fascicularis*. J Comp Neurol 379:113–132.
Mody I, de Koninck Y, Otis TS, Soltesz I (1994) Bridging the cleft at GABA synapses in the brain. Trends Neurosci 17:517–525.
Niedermeyer E, Lopes da Silva F (1993) Electroencephalography: basic principles, clinical applications and related fields. Baltimore: Williams and Wilkins.
Porter JT, Cauli B, Staiger JF, Lambolez B, Rossier J, Audinat E (1998) Properties of bipolar VIPergic interneurons and their excitation by pyramidal neurons in the rat neocortex. Eur J Neurosci 10:3617–3628.
Reyes A, Lujan R, Rozov A, Burnashev N, Somogyi P, Sakmann B (1998) Target-cell-specific facilitation and depression in neocortical circuits. Nat Neurosci 1:279–285.
Salmelin R, Hamalainen M, Kajola M, Hari R (1995) Functional segregation of movement-related rhythmic activity in the human brain. NeuroImage 2:237–243.
Singer W (1993) Synchronization of cortical activity and its putative role in information processing and learning. Annu Rev Physiol 55:349–374.
Singer W, Gray CM (1995) Visual feature integration and the temporal correlation hypothesis. Annu Rev Neurosci 18:555–586.
Sloper JJ, Powell TPS (1978) Dendro-dendritic and reciprocal synapses in the primate motor cortex. Proc R Soc Lond B Biol Sci 203:23–38.
Somogyi P, Cowey A (1981) Combined Golgi and electron microscopic study on the synapses formed by double bouquet cells in the visual cortex of the cat and monkey. J Comp Neurol 195:547–566.
Somogyi P, Tamás G, Lujan R, Buhl EH (1998) Salient features of synaptic organisation in the cerebral cortex. Brain Res Rev 26:113–135.
Steriade M, McCormick DA, Sejnowski TJ (1993) Thalamocortical oscillations in the sleeping and aroused brain. Science 262:679–685.
Steriade M, Amzica F, Contreras D (1996) Synchronization of fast (30–40 Hz) spontaneous cortical rhythms during brain activation. J Neurosci 16:392–417.
Tamás G, Buhl EH, Somogyi P (1997) Fast IPSPs elicited via multiple synaptic release sites by distinct types of GABAergic neuron in the cat visual cortex. J Physiol (Lond) 500:715–738.
Tamás G, Somogyi P, Buhl EH (1998) Differentially interconnected networks of GABAergic interneurons in the visual cortex of the cat. J Neurosci 18:4255–4270.
Tamás G, Buhl EH, Lorincz A, Somogyi P (2000) Proximally targeted GABAergic synapses and gap junctions synchronize cortical interneurons. Nat Neurosci 3:366–371.
Traub RD, Whittington MA, Stanford IM, Jefferys JGR (1996) A mechanism for generation of long-range synchronous fast oscillations in the cortex. Nature 383:621–624.
Venance L, Rozov A, Blatow M, Burnashev N, Feldmeyer D, Monyer H (2000) Connexin expression in electrically coupled postnatal rat brain neurons. Proc Natl Acad Sci USA 97:10260–10265.